Impact of external carbon dose on the removal of micropollutants using methanol and ethanol in post-denitrifying Moving Bed Biofilm Reactors

Torresi, Elena; Escolà Casas, Mònica; Polesel, Fabio; Plósz, Benedek G.; Christensson, Magnus; Bester, Kai

Published in:
Water Research

Link to article, DOI:
10.1016/j.watres.2016.10.068

Publication date:
2017

Document Version
Peer reviewed version

Impact of external carbon dose on the removal of micropollutants using methanol and ethanol in post-denitrifying Moving Bed Biofilm Reactors

Elena Torresi[† 1,2], Mònica Escolà Casas[† 3], Fabio Polesel[2], Benedek G. Plósz[2*], Magnus Christensson[1*], Kai Bester[3*]

[†] *Joint first authors; * Corresponding authors: kb@dmu.dk; magnus.christensson@anoxkaldnes.com; beep@env.dtu.dk;*

[1] Veolia Water Technologies AnoxKaldnes, Klosterängsvägen 11A, SE-226 47 Lund, Sweden

[2] Department of Environmental Engineering, Technical University of Denmark, Bygningstorvet B115, 2800 Kgs. Lyngby, Denmark

[3]Department of Environmental Science, Århus University, Frederiksborgvej 399, 4000 Roskilde, Denmark

Keywords: pharmaceuticals; MBBR; carbon source; biofilms; wastewater; denitrification

Abstract

Addition of external carbon sources to post-denitrification systems is frequently used in wastewater treatment plants to enhance nitrate removal. However, little is known about the fate of micropollutants in post-denitrification systems and the influence of external carbon dosing on their removal. In this study, we assessed the effects of two different types and availability of commonly used carbon sources —methanol and ethanol— on the removal of micropollutants. Two laboratory-scale moving bed biofilm reactors (MBBRs), containing AnoxKaldnes K1 carriers with acclimated biofilm from full-scale systems, were operated in continuous-flow using wastewater dosed with methanol and ethanol. Batch experiments with 22 spiked pharmaceuticals were performed to assess removal kinetics. Acetyl-sulfadiazine, atenolol, citalopram, propranolol and trimethoprim were easily biotransformed in both MBBRs (biotransformations rate constants k_{bio} between 1.2 and 12.9 L $g_{biomass}^{-1}$ d^{-1}), 13 compounds were moderately biotransformed (rate constants between 0.2 and 2 L $g_{biomass}^{-1}$ d^{-1}) and 4 compounds were recalcitrant. The methanol-dosed MBBR showed higher k_{bio} (e.g., 1.5 to 2.5-fold) than in the ethanol-dosed MBBR for 9 out of the 22 studied compounds, equal k_{bio} for 10 compounds, while 3 compounds (i.e., targeted sulfonamides) were biotransformed faster in the ethanol-dosed MBBR. While biotransformation of most of the targeted compounds followed first-order kinetics, removal of venlafaxine, carbamazepine, sulfamethoxazole and sulfamethizole could be described with a cometabolic model. Analyses of the microbial composition in the biofilms using 16S rRNA amplicon sequencing revealed that the methanol-dosed MBBR contained higher microbial richness than the one dosed with ethanol, suggesting that improved biotransformation of targeted compounds could be associated with higher microbial richness. During continuous-flow operation, at conditions representative of full-scale denitrification systems (hydraulic residence time = 2 h), the removal efficiencies of micropollutants were below 35% in both MBBRs, with the exception of atenolol and trimethoprim (>80%). Overall, this study

43 demonstrated that MBBRs used for post–denitrification could be optimized to enhance the
44 biotransformation of a number of micropollutants by accounting for optimal carbon sources and
45 extended residence time.
46

1. Introduction

Currently used biological processes in conventional wastewater treatment plants (WWTPs) are designed to remove organic carbon and nutrients (nitrogen and phosphorus). As organic micropollutants are gaining attention due to the associated environmental risks (Daughton and Ternes, 1999; Plósz et al., 2013), the optimization of biological processes for removal of micropollutants during wastewater treatment is crucial (Joss et al., 2008). Micropollutants (e.g., pharmaceuticals and personal care products) are generally recognized as non-growth substrates (secondary substrates), as they are present in wastewater in too low concentrations (ng L^{-1} to µg L^{-1}) to support biomass growth (Fischer and Majewsky, 2014; Rittmann, 1992). Therefore, biological transformation of micropollutants is mainly the result of cometabolic mechanisms, whereby the removal of non-growth substrates (micropollutants) requires the presence of primary substrates (i.e., COD, nutrients) to support biomass growth (Criddle, 1993; Rittmann, 1992). In cometabolism, the biotransformation of micropollutant is typically catalyzed by non-specific enzymes (e.g., mono- or di-oxygenases, *N*-acetyltransferases, hydrolases) or by cofactors produced during the microbial conversion of the primary substrate (Criddle, 1993; Fischer and Majewsky, 2014). Nevertheless, the interaction between primary substrate and micropollutants is complex and not completely understood. In fact, the presence of primary substrate has been reported to either enhance the removal of micropollutants, e.g., by regenerating reductants such as NAD(P)H under aerobic conditions (Alvarez-Cohen and Speitel, 2001; Liu et al., 2015), or decrease it, due to competitive enzyme inhibition (Fischer and Majewsky, 2014; Plósz et al., 2010).

Recent studies have proposed biofilm systems, e.g., moving bed biofilm reactors (MBBR), as a promising alternative to activated sludge systems (CAS) with respect to the attenuation of micropollutants (Escolà Casas et al., 2015a; Falås et al., 2012; Hapeshi et al., 2013; Torresi et al.,

2016). In general, most of the studies concerning the removal of micropollutants during biological wastewater treatment have focused on aerobic systems, whereas only little information is available for anoxic denitrifying conditions: Plósz et al., 2010; Su et al., 2015; Falås et al. 2013, Suárez et al., 2010. While pharmaceuticals such as diclofenac, metoprolol, erythromycin and roxithromycin were found to be transformed mainly under aerobic conditions in activated sludge using synthetic wastewater (Suárez et al., 2010) and in hybrid biofilm-activated sludge processes (Falås et al., 2013), some of the investigated chemicals had similar (i.e., bezafibrate, atenolol, clarithromycin and N^4-acetylsulfamethoxazole) or higher (i.e., levetiracetam) biotransformation under anoxic conditions than under aerobic ones (Falås et al., 2013). Hence, anoxic biological processes in conventional WWTPs should be considered as a potential step to optimize removal of micropollutants.

The type of carbon source is known to have a strong impact on the structure of denitrifying microbial communities and thus on denitrification efficiency (Baytshtok et al., 2009; Hagman et al., 2007; Lu et al., 2014). This has specific relevance to post-denitrification reactors in full-scale WWTPs, where nitrate removal is achieved by dosing external carbon sources such as methanol and ethanol (Louzeiro et al, 2002; Santos et al., 2001). Methanol and ethanol are metabolized by denitrifying bacteria through different pathways. Methanol undergoes the metabolic reaction of single-carbon compounds, which is exclusive to methylotrophs because of their unique key enzyme (methanol dehydrogenase) that catalyzes the oxidization of methanol to formaldehyde (Anthony et al., 1982, 2011). Instead, ethanol is easily converted by bacterial cells to Acetyl-CoA before entering the glyoxylate cycle (Anthony et al., 2011). Thus, microbial communities in post-denitrifying systems using either of these carbon sources may be fundamentally different and potentially exhibit a different biodiversity and functionality with more or less microbial specialists able to biotransform organic micropollutants. Additionally, biodiversity in terms of species richness

(the number of species) and evenness (the relative abundance of the species) (Wittebolle et al., 2009) was shown to positively associate with the biotransformation of a number of micropollutants in aerobic activated sludge (Johnson et al., 2015; Stadler and Love, 2016) and nitrifying MBBRs (Torresi et al., 2016). Further investigation of the impact of biodiversity in different biological treatment systems seems thus required.

In this study, we evaluated the elimination of selected micropollutants (i.e., pharmaceuticals) in laboratory-scale post-denitrifying MBBRs dosed with methanol or ethanol. Biotransformation kinetics and removal efficiencies were assessed through targeted batch experiments and during continuous-flow MBBR operation, respectively. The objectives of our study were: (i) to investigate the impact of different types of external carbon sources (methanol and ethanol) for post-denitrification on micropollutant biotransformation; (ii) to assess the structure of the denitrifying microbial community of MBBR biofilms, following continuous dosing with either methanol or ethanol; and (iii) to evaluate the influence of organic substrate availability on the transformation of micropollutants and the related mechanisms, i.e. competitive inhibition and cometabolic enhancement.

2. Materials and Methods

2.1 Description of the post-denitrifying systems

Two Swedish WWTPs, i.e., Sjölunda and Klagshamn are currently dosing methanol or ethanol, respectively, as external carbon source in two-stage post-denitrification MBBRs. Thus, two laboratory-MBBRs were built to resemble such post-denitrification stages, using carriers (AnoxKaldnes K1) from the first post-denitrification tank of the respective WWTPs already adapted to methanol and ethanol dosing. The WWTPs are described in Section S1 of the SI (Supporting

Information). Both laboratory-MBBRs (1 L) were operated in continuous feeding of the same wastewater, which was collected after the (aerobic) nitrification step (trickling filter) of Sjölunda WWTP (Lund, Sweden). Thus, during continuous-flow operation, only the indigenous nitrate and nitrite present in the wastewater (averaged concentration of 13 and 1.2 mg L^{-1} respectively) were used for denitrification. The filling rate of both reactors was 40%, giving a surface of 0.2 m^2. The amount of indigenous micropollutants in the reactor influents (consisting in the collected wastewater and feed containing carbon-source) was analyzed. Twelve compounds were quantified giving concentrations between 0.04 µg L^{-1} (trimethoprim) and 78 µg L^{-1} (iohexol). Complete details of these results are given in Table S6 (SI).

The reactors were continuously flushed with nitrogen gas and stirred for the mixing of the carriers and to strip eventual residual dissolved oxygen. Both reactors were kept at 15°C using a water bath. The feed wastewater was mixed and kept at 4°C during the whole experiment. Phosphate was added to the feed to reach a concentration of 0.5 mg L^{-1} to ensure biofilm growth on the carriers. Micropollutant removal and denitrification rates in MBBRs were assessed in two main experiments: (i) batch conditions (24 h) and (ii) continuous-flow operation (2 months). The carbon availability of ethanol and methanol into the two MBBRs was defined as the ratio between the influent loading of organic carbon (COD_{added}) and the native loading of nitrate (NO_3-$N_{influent}$) in the wastewater samples. Optimum COD_{added}/NO_3-$N_{influent}$ ratio (gCOD gN^{-1}) for complete denitrification is typically around 4 (Metcalf & Eddy, 2003).

2.2 Analytical methods

All the samples taken for analysis of conventional pollutants (NH_4^+-N, NO_3^--N, NO_2^--N, soluble COD and PO_3^{4-}) in batch and continuous experiments were filtered through 0.45 µm glass fiber

filters (Sartorius, Göttingen, Germany). Total COD and total nitrogen were analyzed on the unfiltered sample. All samples were prepared in Hach Lange kits (LCK 303, LCK 339, LCK 341 and LCK 342) and analyzed in a Hach Lange DR2800 spectrophotometer. DO, pH and temperature in the reactors were measured at each sampling occasion, using a Hach HQ40d multi DO probe and a HANNA H1991001 pH-meter. The attached biomass concentrations were calculated from the difference in weight of 3 dried carriers (105 °C for >24 h) before and after biofilm removal (in 2M H_2SO_4) with subsequent brushing (see Figure S2 for results), as previously considered (Escolà Casas et al., 2015a; Falås et al., 2012; Torresi et al., 2016). Samples for micropollutants were frozen at -20 ^{o}C prior analysis and analyzed via direct injection using HPLC-MS/MS as described in Escolà Casas et al. (2015a). Information regarding sample preparation, HPLC, mass spectrometry data, LOD and LOQ of compounds are shown in Escolà Casas et al. (2015a) and in Section S2 (SI).

2.3 Chemicals

Twenty-two relevant micropollutants (i.e., pharmaceuticals) were selected for this study. Information regarding CAS numbers and chemical suppliers is found in the supplementary information in Escolà Casas et al. (2015b). The pharmaceuticals included: (i) four beta-blockers, i.e., atenolol, metoprolol, propranolol and sotalol; (ii) five X-ray contrast media, i.e., diatrizoic acid, iohexol, iopamidol, iopromide, iomeprol; (iii) three sulfonamides, i.e., sulfadiazine, sulfamethizole and sulfamethoxazole and the metabolite acetyl-sulfadiazine; (iv) three analgesics, i.e., phenazone, diclofenac and ibuprofen; (v) three anti-epileptics/anti-depressants, i.e., carbamazepine, venlafaxine and citalopram; (vi) four antibiotics, i.e., erythromycin, clarithromycin, trimethoprim and roxithromycin.

2.4 Batch experiment

To investigate how the type of dosed carbon source influences the removal of micropollutants in post-denitrifying MBBR, batch experiments were performed in the same reactors used during continuous-flow operation. These experiments were conducted after 3.5 months of continuous-flow operation of the two systems. During the batch experiments, a $COD_{added}/NO_3\text{-}N_{influent}$ ratio of 3.4 for both reactors was adopted to obtain excess concentration of nitrate. Anoxic conditions were maintained by flushing the reactors with nitrogen gas during the experiment. The feed used for the batch consisted of the same wastewater used in continuous operation spiked with 239 ± 2 mg COD L^{-1} of methanol for the methanol-dosed reactor and the same amount of ethanol for the ethanol-dosed reactor, 70 ± 3 mg NO_3-N L^{-1} in form of sodium nitrate and 22 micropollutants with an initial nominal concentration of 2 μg L^{-1}. The micropollutants were added from a stock solution (40 mg L^{-1} in methanol). To minimize the increase of COD concentration in the batch feed due to the methanol from the stock solution, the micropollutant solution was first spiked into an empty glass beaker and the methanol was let to evaporate for approximately 1 hour. Afterwards, the feed was added to the beaker containing the micropollutants and mixed to re-dissolve the micropollutants. The batch experiment lasted 24 hours and samples for conventional and micropollutants analysis were taken at regular intervals. To keep the biomass concentration constant during the experiment, three carriers were withdrawn from the reactors each time a sample was taken for analysis. The pH value in both reactors was continuously measured and adjusted to 7.5 using 1M HCl. The temperature was kept constant at 15°C.

2.4.1 Denitrification during batch experiment

Denitrification rates normalized on surface area of reactors $r_{NO3,2\text{-}N}$ ($gNO_{3,2}$-N m^{-2} d^{-1}) and specific denitrification rates accounting for the biomass $kNO_{3,2}$-N ($gNO_{3,2}$-N $g_{biomass}^{-1}$ d^{-1}) were derived

through linear regression using NO_3^--N and NO_2^--N measurements during batch experiment. An accumulation of nitrite in the systems was noticed (~ 6 mg L^{-1}), therefore $NO_{3,2}$-N utilization curves accounting also for NO_2^--N concentration were derived accordingly to Sözen et al. (1998).

A two step-denitrification activated sludge model (ASM) was used to describe up-take of primary substrates (i.e., readily soluble biodegradable COD (S_S), soluble nitrate (S_{NO3}) and nitrite (S_{NO2})) which was extended with the Activated Sludge Model for Xenobiotics ASM-X (Plósz et al., 2012; Polesel et al., 2016) to determine micropollutant biotransformation rates (Table 1). Readily soluble biodegradable COD (S_S) was determined as the difference between soluble COD (sCOD)—measured during the experiments—and soluble inert COD (S_I)—calculated according to Roeleveld and Van Loosdrecht (2002). The ASM for denitrification was adapted from Pan et al. (2015) and included two process rate equations with reduction of nitrate to nitrite (R1) and nitrite to nitrogen (R2) (Table 1). Parameters that could not be identified through model calibration to experimental results (maximum specific growth rates μ_H, affinity constants for substrate—K_{S1} and K_{S2}—and for nitrogen species—K_{NO3}^{HB} and K_{NO2}^{HB} —) were adopted from literature (Hiatt and Grady, 2008). Parameters that are known to be sensitive to the experimental data (i.e., heterotrophic yields Y_H, anoxic growth factors for the process 1 and 2, η_{g1} and η_{g2}) were calibrated. Definition of the components and model calibration are presented in Section S3 and Table S1 (SI). The model was implemented in AQUASIM 2.1d (Reichert et al., 1994) and the parameters were estimated using the secant method embedded.

2.4.2 Micropollutants removal kinetics during batch experiment

Model structures to assess biotransformation rate of micropollutants were identified using the ASM-X as modelling framework (Polesel et al., 2016; Plósz et al., 2010, 2012, 2013). The framework

used in this study is summarized in Table 1 and included processes such as parent compound retransformation (e.g., deconjugation of human metabolites) (1), biotransformation (2) and cometabolic biotransformation (in the presence and absence of organic growth substrate) (3). The effect of diffusion into biofilm on the removal of pharmaceuticals from bulk aqueous phase was lumped in the biotransformation rate constants, as previously considered by Falås et al. (2012, 2013), Escolá Casas et al. (2015a) and Hapeshi et al. (2013). The cometabolic process was modelled as proposed by Plósz et al. (2012), using pseudo-first order kinetics with respect to micropollutant concentration and estimating two biokinetics: (i) the cometabolic biotransformation rate constant q_{bio} in the presence of the primary substrate and (ii) biotransformation rate constant k_{bio} in the absence of primary substrate. Accordingly, biotransformation kinetics of the cometabolic substrate (e.g., micropollutant) depend on the primary substrate concentration (e.g., organic matter expressed as readily soluble biodegradable COD, S_S) considered a co-limiting substrate. In Table 1 C_{LI} and C_{CJ} denote the aqueous concentration (ng L^{-1}) of the parent compound and the human metabolites undergoing deconjugation to the parent compound, respectively. The retransformation rate constant k_{Dec} (L $g_{biomass}^{-1}$ d^{-1}) defines kinetics of retransformation to parent compound. Sorption processes were also included considering the sorption coefficient K_D (L $g_{biomass}^{-1}$) which was calibrated using values from previous studies estimated under denitrifying condition when available (Table S2 in SI). As to the best of our knowledge values of K_D were not previously estimated for biofilm under denitrifying conditions, K_D measured for activated sludge were used in this study. The half-saturation coefficient for S_S, (K_S) in Table 1, was retrieved from Hiatt and Grady (2008). $X_{biomass}$ ($g_{biomass}$ L^{-1}) denoted the biomass concentration in the MBBRs and growth of biomass on micropollutants was considered negligible.

Biotransformation constants k_{bio} (process 2, Table 1) were estimated from the measured data using least-square optimization without weighting in GraphPad Prism 5.0. Parent compound retransformation and cometabolism model (processes 1 and 3, Table 1) were implemented in AQUASIM 2.1d (Reichert et al., 1994) and the parameters were estimated using the secant method embedded.

Removal rate constants k (d^{-1}) were also estimated to compare the performance of the two MBBR systems, regardless of biomass concentration and sorption processes (Escolà Casas et al., 2015a,b). For the chemicals following cometabolism model (and thus exhibiting two biokinetics), k was calculated considering the estimated q_{bio}. Differences between biotransformation rate constants of the two MBBRs were assessed by examining the overlap between standard deviations of the estimated values (Cumming et al., 2007).

2.5 DNA extraction, PCR amplification, sequencing and bioinformatics analysis.

One carrier was collected from each MBBR before the batch experiment and stored in a sterilized Eppendorf tube at -20 ^{o}C. Biomass was detached using a sterile brush (Gynobrush, Dutscher Scientific, United Kingdom) using tap water and consequently centrifuged (10000 rpm for 5 minutes) to remove excess water. DNA extraction, PCR amplification (using 16S rRNA bacteria gene primers) and Illumina sequencing were performed as described in Section S5 of the SI. Taxonomic assignment and calculation of alpha diversity metrics (Shannon biodiversity and ACE extrapolated richness) were performed in mothur using the RDP reference taxonomy. Additional diversity indices were calculated according to Hill et al. (1973). Microbial evenness was estimated as H_1/H_0 as described in Johnson et al. (2015).

2.6 Continuous-flow experiment

The two MBBRs used for the present study were operated for over 4 months. The MBBRs were kept with a $COD_{added}/NO_3\text{-}N_{influent}$ ratio equal to 3 (close to the ratios used at the respective WWTPs) for the first two weeks of operation. The fraction of inert COD was taken into account (by subtracting it from the amount of available biodegradable COD) when planning experiments under carbon limitation. A hydraulic retention time (HRT) of 2 hours was set similar to the HRT used at the full-scale WWTPs. After two weeks of acclimatization, baseline carbon-dosage periods of $COD_{added}/NO_3\text{-}N_{influent}$ were alternated with short carbon-dosage periods (~5 days) to avoid biomass adaptation. Accordingly, concentrations of methanol and ethanol in the feed solutions were changed to test $COD_{added}/NO_3\text{-}N_{influent}$ ratios ranging from 1 to 5, while keeping constant HRT. This test phase lasted about 2 months. The $COD_{added}/NO_3\text{-}N_{influent}$ ratios and the dates are reported in the Table S3 (SI). The range of $COD_{added}/NO_3\text{-}N_{influent}$ ratios was chosen to assess carbon limiting condition at low $COD_{added}/NO_3\text{-}N_{influent}$ ratio and not far exceeding the stoichiometric $COD_{added}/NO_3\text{-}N_{influent}$ ratio needed for complete denitrification. The denitrification rate r_D (gN d^{-1} m^{-2}) in continuous operation, was calculated for each carbon-dosage test by using the Equation S1 (Section S6, SI). Micropollutant removal efficiency ("measured removal" in Figure 4) was calculated as difference between inlet and outlet concentrations. Micropollutant removal efficiency during continuous operation ("predicted removal" in Figure 4) was predicted using removal rate constant k (d^{-1}) estimated during batch experiment according to Equation 1:

$$Removal\ (\%) = \left(1 - \left(\frac{1}{(1+k_i \cdot HRT)}\right)\right) \cdot 100 \qquad \text{Equation 1}$$

3. Results and discussion

3.1 Batch experiment

3.1.1 Denitrification kinetics

Denitrification rates ($r_{NO3,2-N}$, $k_{NO3,2-N}$) were derived through linear regression of measured NO_3^--N and NO_2^--N concentration during batch experiment (Figure S5, SI). The ethanol-dosed reactor presented a higher surface-normalized denitrification rate $r_{NO3,2-N}$ (Table 2) than the methanol driven one, which is in agreement with previous studies (Santos et al., 2001; Christensson et al., 1994). This is likely due to the higher growth yield expected using ethanol thereby leading to higher biomass production per surface area in ethanol-dosed systems (Mokhayeri et al., 2009). On the other hand, denitrification rates ($k_{NO3,2-N}$) normalized by biomass weight (higher for the ethanol-dosed reactor) were comparable in the two MBBRs, suggesting similar activity in terms of nitrate and nitrite removal in the two biofilms.

3.1.2 Micropollutant removal kinetics

Biotransformation kinetics of most of the investigated chemicals could be described with first-order equation (Table 1, process 2), thereby allowing for the estimation of removal rates k (d^{-1}) and pseudo-first order biotransformation rate constants k_{bio} (L $g_{biomass}^{-1}$ d^{-1}). Abiotic transformation processes were previously investigated by the authors using plastic (polyethylene) carriers (AnoxKaldnes Z-carriers) and effluent wastewater (Torresi et al., 2016), suggesting no significant impact of abiotic processes (e.g., abiotic hydrolysis, volatilization, sorption onto plastic or glass) on the removal of several targeted micropollutants (Figure S9). Figures 1 and S1 summarize measured and simulated micropollutant concentration profiles during batch experiments.

306 The removals of erythromycin, clarithromycin, venlafaxine, carbamazepine, sulfamethoxazole and
307 sulfamethizole was predicted using (i) a pseudo-first order biotransformation model (Table 1,
308 process 2), with no interaction (inhibition/enhancement) between micropollutant and primary
309 substrate; and (ii) additionally, a cometabolic model (Table 1, process 3), assuming that the
310 turnover of the micropollutants is enhanced by the presence of primary substrate. Predictions with
311 the two models are presented in Figure 1b–d using dashed lines and solid lines, respectively. The
312 goodness of the two model fits (R^2) is summarized in Table S4 (SI). For erythromycin and
313 clarithromycin, the cometabolic model ($R^2 > 0.9$) provided only for a marginal improvement of the
314 fitting compared to the pseudo-first order biotransformation model ($R^2 > 0.8$), making it difficult to
315 draw conclusion on the removal mechanism of these two compounds. However, the prediction of
316 carbamazepine's removal was significantly improved by adopting the cometabolic model ($R^2 > 0.9$)
317 compared to the pseudo first-order biotransformation model ($R^2 < 0.5$) in both MBBRs.
318 Cometabolic biotransformation of carbamazepine has been previously observed in aerobic and
319 anoxic activated sludge (Plósz et al., 2012) with cometabolic biotransformation rate constant q_{bio}
320 (1.2 L g^{-1} d^{-1} under anoxic condition), in close agreement with our results. Similarly, the removal of
321 venlafaxine, sulfamethoxazole and sulfamethizole removal was better predicted using the
322 cometabolic model ($R^2 > 0.9$). In Figure 1a, the measured and simulated concentration of soluble
323 COD (sCOD), nitrate (NO_3-N) and nitrite (NO_2-N) and simulated readily biodegradable COD (S_S)
324 are reported. For the abovementioned micropollutants, S_S limitation (approximately after 3 hours
325 from the beginning of the experiment) corresponded to a change in biotransformation kinetics.
326 Interestingly, in the ethanol-fed reactor, the modelled S_S limitation coincided with a significant
327 decrease in the biotransformation rates of sulfamethoxazole and sulfamethizole (Figure 1d right),
328 thereby leading to a rather low removal rate during the rest of the experiment. A similar effect for
329 both compounds, though at lower extent, was observed for the methanol-dosed reactor.

Cometabolic transformation of trace chemicals was previously shown in suspended cultures under aerobic, anaerobic and anoxic conditions (Delgadillo-Mirquez et al., 2011; Fernandez-Fontaina et al., 2014; Plósz et al., 2010; Popat and Deshusses, 2011; Tran et al., 2013). Removal via cometabolism was previously observed for sulfamethoxazole in nitrifying (Kassotaki et al., 2016; Müller et al., 2013) and in aerobic and anoxic activated sludge (Alvarino et al., 2016), as well as for erythromycin and roxithromycin (Fernandez-Fontaina et al., 2014) in nitrifying activated sludge. Thus, our results support the hypothesis that the change of primary substrate availability can significantly impact the removal of a number of micropollutants as a result of cometabolic mechanisms under denitrifying conditions.

While the other sulfonamides followed cometabolic biotransformation, the removal of sulfadiazine was different. It could not be described with first-order kinetics ($R^2 < 0.2$ and < 0.4 for methanol- and ethanol-dosed MBBR respectively, dashed lines in Figure 1 e), due to the presence of its conjugate acetyl-sulfadiazine. Acetyl-sulfadiazine is the main human metabolite of sulfadiazine (Vree et al., 1995) and it has been previously observed to undergo de-acetylation (Zarfl et al., 2009), similarly to other acetyl-sulfonamides such as N^4-acetylsulfamethoxazole (Göbel et al., 2007). For these chemicals, a model including retransformation (deconjugation) of acetyl-sulfadiazine to sulfadiazine and concurrent biotransformation of sulfadiazine was used to estimate biotransformation rate constants k_{bio} for sulfadiazine and retransformation rate constant k_{Dec} for acetyl-sulfadiazine (Table 1, processes 1 and 2). However, this modelling approach did not adequately describe the concentration changes of sulfadiazine in any of the MBBRs ($R^2 < 0.2$, continuous lines in Figure 1e):

For the methanol-dosed MBBR, acetyl- sulfadiazine was decreasing rapidly and sulfadiazine (being formed from acetyl-sulfadiazine) reached a maximum before being slowly further biotransformed

(Figure 1e left). In the ethanol-dosed MBBR, the acetyl-sulfadiazine was also rapidly removed and sulfadiazine concentration did never increase. Thus, for the ethanol-dosed reactor there is no indication for a deconjugation reaction of acetyl-sulfadiazine to sulfadiazine, while that is partially possible in the methanol-dosed one. Hence, the transformation of acetyl-sulfadiazine probably occurred partially following another metabolic pathway leading to the formation of other (undetected) transformation products. To test whether other pathways could be possible, the EAWAG-BBD pathway prediction systems (EAWAG-BBD, 2016) was used: It showed the possible transformation of acetyl-sulfadiazine to other transformation products, e.g., 2-aminopyrimidine and 4-aminobenzenesulfonic acid (Figure S6, SI). However, additional research on the different transformation pathways of acetyl-sulfadiazine in the two tested MBBRs is needed to substantiate this hypothesis. Further discussion on the biotransformation of acetyl-sulfadiazine and sulfadiazine in the two investigated MBBRs is reported in S4 in SI.

3.2. Influence of dosed carbon-source on microbial communities

We analyzed the biofilm microbial community of the two different MBBRs by 16S rRNA amplicon sequencing. After implementation of quality control measures, a total of 10847 high quality sequences were obtained with an average length of 460 bp. Subsequently, the number of reads of each sample was normalized to 4562 sequences and clustered into an average of 690 observed OTUs at 97% sequence similarity per sample (cut-off level of 3%). The facultative methanol-utilizing β-Proteobacteria, *Methylophilus*, was identified as the main relative abundance genus (24%) in the methanol-dosed reactor (Figure 2)—a result that closely agreed with previous studies on methanol-dosing denitrification systems (Baytshtok et al., 2009; Jenkins et al., 1987; Lu et al., 2014). For the biofilm grown in the ethanol-dosed reactor, *Arcobacter* and *Thiothrix* genus exhibited 23% and 9% relative abundance, respectively. *Arcobacter* was previously identified in

379 full-scale MBBRs treating municipal wastewater (Biswas and Turner, 2012). *Thiothrix* is known to
380 degrade sulfur containing compounds and it was suggested to influence the removal of sulfa-based
381 antibiotics in membrane bioreactors (Xia et al., 2012). Microbial community diversity in the two
382 MBBRs was evaluated by comparing Shannon diversity and evenness indices. We observed no
383 major difference in the methanol- and ethanol-dosed reactors between Shannon diversity indices
384 (4.153 ± 0.05 and 4.184 ± 0.03, mean and standard deviation, respectively) and evenness (0.092 ±
385 0.002 and 0.095 ± 0.001, respectively) (Figure 2, Table S5 of the SI). Similar values of Shannon
386 diversity indices were found previously in aerobic nitrifying MBBRs (Bassin et al., 2015; Torresi et
387 al., 2016). On the other hand, the extrapolated taxonomic richness ACE in the methanol- and
388 ethanol-dosed reactors were estimated to be 999 ± 103 and 781 ± 87 OTUs, respectively, thus
389 suggesting slightly differences between the microbial richness of the two biofilms (Figure 2).
390 Similar evidence was obtained from nitrite reductase *nirK*- and *nirS*-based restriction fragment
391 length polymorphism (RFLP) analysis on activated sludge supplemented with methanol or ethanol,
392 with higher diversity in terms of richness of *nirS* genotypes observed in the methanol-dosed sludge
393 (Hallin et al., 2006).
394
395 **3.3. Influence of dosed carbon source on micropollutants biotransformation**
396 A comparative assessment of the estimated k_{bio}, q_{bio} and k_{Dec} values for the methanol- and ethanol-
397 dosed MBBRs is shown in Figure 3. For 9 compounds the estimated values of biotransformation
398 and cometabolic transformation rate constants (k_{bio} and q_{bio}) for the methanol-dosed MBBR were
399 higher (1.5 to 2.5-fold) than those from the ethanol-dosed reactor (namely atenolol, citalopram,
400 trimethoprim, ibuprofen, iopromide, metoprolol, iohexol, iomeprol, sotalol, venlafaxine).
401 Conversely, the sulfonamides acetyl-sulfadiazine, sulfamethoxazole, sulfamethizole were
402 transformed at higher rate constants (up to 2.8-fold) in the ethanol-dosed reactor. The remaining 10

403 compounds behaved similarly in both reactors. We further classified the biotransformation potential
404 of the targeted micropollutants of the two denitrifying MBBRs in three groups (Table 3): easily
405 degradable (q_{bio} and $k_{bio} > 2$), moderately degradable ($0.2 \leq k_{bio}$ and $q_{bio} \geq 2$) and hardly degradable
406 (k_{bio} and $q_{bio} < 0.2$).
407 We observed that some of the targeted chemicals classified as easily degradable (propranolol,
408 atenolol, citalopram) presented removal rate constant k (d^{-1}) above 10 d^{-1} and similar between the
409 two MBBRs (Table 3). As the two MBBRs presented different amount of biomass (Table 2) during
410 batch experiment, the lower values of k_{bio} for the high degradable compounds in the ethanol-dosed
411 reactor could mainly derive from the normalization to a higher amount of biomass prevailing in the
412 ethanol-dosed reactor.
413 On the other hand, a number of moderately degradable chemicals (i.e., X-ray contrast media,
414 ibuprofen, metoprolol and sotalol) were associated to k and k_{bio} values approximately two times
415 higher in the methanol-dosed than in the ethanol-dosed reactor. The two biofilm microbial
416 communities likely played an important role on the biotransformation of these chemicals. As
417 previously described (Section 3.2), the higher microbial richness observed in the biofilm enriched
418 with methanol could have likely contributed to the overall higher micropollutant biotransformation
419 in the methanol-dosed MBBR. Similarly, positive associations between biodiversity and the rates of
420 specific micropollutant biotransformations were observed in activated sludge (Johnson et al., 2015;
421 Stadler and Love, 2016) and MBBR (Torresi et al., 2016).
422 No major differences were observed between the biotransformation rate constants k_{bio} of the hardly
423 degradable compounds (diatrizoic acid, iopamidol, diclofenac and phenazone) in the two MBBRs,
424 suggesting that their removal is neither biomass nor carbon source dependent.
425

3.4 Highlighted compounds

Among the X-ray contrast media, iopamidol and diatrizoic acid were found to be recalcitrant in both reactors during batch experiment (Figure S1, SI), while iomeprol, iohexol and iopromide were found moderately degradable (Figure 1d). These results are in agreement with previous studies conducted with aerobic MBBRs (Escolà Casas et al., 2015a; Hapeshi et al., 2013). Our results show that denitrifying MBBRs could effectively remove iomeprol, iohexol and iopamidol, with k_{bio} comparable to studies on activated sludge (Joss et al., 2006; Onesios et al., 2009)

The analgesic ibuprofen exhibited lower biotransformation rate constants (Table 3) than the ones obtained in previous studies under aerobic conditions (Escolà Casas et al., 2015a,b; Falås et al., 2012; Torresi et al., 2016) as ibuprofen is easily degraded under aerobic conditions. Other analgesics, i.e., phenazone and diclofenac, have also previously observed to be hardly degradable in both aerobic MBBR and activated sludge (Escolà Casas et al., 2015a; Joss et al., 2006). Nevertheless, k_{bio} values for diclofenac were reported to be higher under nitrifying conditions in both biofilms and activate sludge (Torresi et al., 2016; Tran et al., 2009) than as obtained in this study under denitrifying conditions, thus indicating limited diclofenac removal under anoxic conditions.

In the batch experiment, citalopram was fully removed in both reactors within 0.4 days (Figure 1b), resulting in a k_{bio} of 2.3 L d^{-1} $g_{biomass}^{-1}$ (Table 3). Similar biotransformation kinetics was found in aerobic MBBR (Escolà Casas et al., 2015a) and sludge (Suárez et al., 2012), while anoxic CAS showed lower kientics compared to the one obtained in th anoxic MBBRs of this study. At HRTs higher than 0.4 days, a removal efficiency of 65% was achieved in a complete autotrophic nitrogen removal process (Alvarino et al., 2015). In our study, predicted removal efficiency of citalopram (at HRT of 0.4 days) was calculated to be >80% in both reactors (Equation 1) during continuous-flow

operation. Furthermore, in denitrifying activated sludge reactors a k_{bio} of 0.5 L d^{-1} $g_{biomass}^{-1}$ was obtained for citalopram (Suárez et al., 2010) and a removal of 44 % under anoxic condition (Suárez et al., 2010).

The removal of carbamazepine and venlafaxine (with q_{bio} ranging between 1.1 and 1.9 L g^{-1} d^{-1}) followed the kinetics described by the cometabolic model in our study, as suggested previously (see Section 3.1.2). With respect to biotransformation kinetics, only one study showed cometabolic biotransformation rate constants of up to 2 L g^{-1} d^{-1} for carbamazepine in aerobic and anoxic activated sludge (Plósz et al., 2012). On the other hand biotransformations rate constants equal to 0.9 L g^{-1} d^{-1} in aerobic MBBR have been reported (Escolà Casas et al., 2015a). In our study we thus observed 30 % removal of carbamazepine during batch experiments, which is in agreement with previous studies on MBBR (Escolà Casas et al., 2015a) and activated sludge (Dawas-Massalha et al., 2014; Luo et al., 2014; Zupanc et al., 2013). Thus, low removal of carbamazepine in the tested MBBRs in batch and continuous-flow experiments may be attributed to the limited transformation in the absence of primary substrates.

The biotransformation of the targeted sulfonamides was enhanced in the ethanol-dosed MBBR (up to 1.8-fold higher). As the ethanol-dosed MBBR showed the highest denitrification rates ($r_{NO3,2-N}$) during the batch experiment, the removal of the targeted sulfonamides may be associated with primary metabolism rather than biofilm composition (i.e., biodiversity). Interestingly, negative correlation between biotransformation kinetics of sulfonamides and biodiversity was also observed in nitrifying MBBRs, and their removal was enhanced at higher nitrification rates in thin biofilms (Torresi et al., 2016). Similarly, the removal of sulfamethoxazole has been previously shown to be dependent on the primary metabolism under anoxic condition in activated sludge, while negligible

effect of primary substrate was observed under nitrifying condition (Alvarino et al., 2016). This indicates that sulfonamide removal may be influenced by primary metabolism in both nitrifying and denitrifying conditions.

Finally, while k_{bio} of clarithromycin and erythromycin was found comparable to studies on aerobic MBBRs (Escolà Casas et al., 2015a), trimethoprim removal occurred with a higher k_{bio} under denitrification conditions than in aerobic MBBRs (Escolà Casas et al., 2015a; Falås et al., 2013).

3.5 Impact of carbon dosing during continuous-flow operation

A continuous-flow experiment tested different dosing conditions of organic carbon in terms of primary substrate (methanol or ethanol) and influent loading (variable $COD_{added}/NO_3\text{-}N_{influent}$ ratio) without adaptation of the biofilm as described in Section 2.6 (details in Section S7, SI). The removal efficiency of micropollutants did not present any correlation with the tested $COD_{added}/NO_3\text{-}N_{influent}$ ratios and did not significantly differ between the two types of carbon sources (Figure S8, SI). Notably, only trimethoprim removal increased with increasing carbon availability in the ethanol-dosed reactor.

Both MBBR systems exhibited denitrification rates directly proportional to the $COD_{added}/NO_3\text{-}N_{influent}$ ratio (Figure S3, SI). However, at $COD_{added}/NO_3\text{-}N_{influent}$ ratios higher than 4.8 and 3.8 for the methanol- and the ethanol-dosed MBBR, respectively, denitrification rates did not increase and similar effluent concentrations of COD were measured for both MBBRs (estimated to be equal to the inert soluble COD in the influent medium) (Figure S4, SI). This indicates that excess COD dosing during continuous-flow operation could have been used for internal storage rather than as primary energy source. This has been previously observed under substrate feast-famine cycles in

continuously operated activated sludge (Beun et al., 2000). Similarly, feast-famine conditions associated to change from high to low $COD_{added}/NO_3\text{-}N_{influent}$ ratio during continuous-flow operation might have influenced the performance of the two post-denitrifying MBBRs in this study.

Furthermore, the continuous-flow operation experiment was carried out at HRT of 2 h, simulating HRTs typically operated in denitrification stages in full scale WWTPs, and which might have been too short to observe differences in the removal of micropollutants. In fact, the batch experiment showed that the removal of most of the targeted micropollutants (with the exception of the compounds removed through cometabolism) continued after 2 h from the start of the experiment (Figure 1), suggesting a possible removal enhancement at higher HRT. Accordingly, the increase of HRT has been found to enhance the removal of a number of micropollutants in activated sludge (Maurer et al., 2007; Petrie et al., 2014) and MBBR (Mazioti et al., 2015).

3.6. Comparison of the batch and the continuous-flow experiment

Figure 4 compares the measured removal efficiencies under continuous –flow operation with the predicted removal efficiencies. The predicted values were calculated using the removal rates (k) estimated in the batch experiment according to first-order kinetics (Table 3). As presented in Figure 4, the removal rates (k) estimated from batch experiments allowed predicting of the elimination of most of the targeted compounds in continuous-flow operation. However, predicted removal efficiencies did not match the measurements for a number of micropollutants, i.e. sulfamethoxazole, carbamazepine, atenolol and trimethoprim. A possible explanation for this discrepancy might be that the removal rates (k) used to predict the removals were obtained by fitting the first order kinetics, while in reality for some compounds cometabolic or deconjugation approaches are more appropriate.

As the biotransformation kinetics of most of the compounds could be described with a first-order equation (Table 1, process 2 and Figure 1), it could be predicted that an HRT of 2 h (0.083 d) would only allow a partial removal of the easily biodegradable compounds (e.g., atenolol, trimethoprim and citalopram) in the continuous-flow experiment (Figure 4). For the compounds following this type of biotransformation kinetics, it could be predicted (Equation 1, Section 2.6) that the increase of the HRT up to 6 hours (0.25 d) would improve the removal efficiency by about 20%, achieving high removals in both reactors (>70%) for all the compounds listed as "easily biodegradable" in Table 3.

4. Conclusions

In order to investigate the removal of micropollutants in denitrifying Moving Bed Biofilm Reactors (MBBRs), two laboratory-scale MBBRs were tested using nitrified effluent wastewater dosed with methanol and ethanol, respectively. The following conclusions have been drawn:

- According to the batch experiment, all targeted micropollutants showed biotransformation rate constants over 0.2 L $d^{-1}g_{biomass}^{-1}$ under denitrifying condition, except for diclofenac, phenazone, diatrizoic acid and iopamidol, which were found to be recalcitrant. Accordingly, it has been suggested that that HRTs of approximately 6 h could considerably enhance the removal of most of the targeted micropollutants.

- The biotransformation rate constants in the methanol-dosed MBBR were 1.5 to 2.5-fold higher than in the ethanol-dosed MBBR for 9 out of the 22 spiked pharmaceutical. Oppositely, the sulfonamides acetyl-sulfadiazine, sulfamethoxazole, sulfamethizole were transformed at higher

546 biotransformation rate constants in the ethanol-dosed MBBR. The rest of the compounds
547 presented similar biotransformation in both reactors.
548
549 • The removal of venlafaxine, carbamazepine, sulfamethoxazole and sulfamethizole was most
550 likely enhanced by the presence of organic growth substrates in the beginning of the batch
551 experiment, suggesting cometabolic removal for these compounds.
552
553 • The continuous-flow experiment conducted at conditions typically operated in full-scale
554 WWTPs (i.e., HRT =2h) did not show significant correlation between the removal efficiency of
555 micropollutants and the increase of carbon dosage or type.
556
557 **5. Acknowledgements**
558 This research was supported by (i) the AUFF grant: advanced water purification using bio-inorganic
559 nanocatalysts and soil filters; and (ii) MERMAID: an Initial Training Network funded by the People
560 Programme (Marie-Curie Actions) of the European Union's Seventh Framework Programme
561 FP7/2007-2013/ under REA grant agreement n. 607492. The authors are thankful for technical
562 assistance provided by VA SYD at Sjölunda and Klagshamn (Malmö) wastewater treatment plants.
563

564 **References**

565

566 Alvarez-Cohen, L., Speitel, G.E., 2001. Kinetics of aerobic cometabolism of chlorinated solvents.
567 Biodegradation 12 (2), 105–126.

568 Alvarino, T., Nastold, P., Suárez, S., Omil, F., Corvini, P.F.X., Bouju, H., 2016. Role of
569 biotransformation, sorption and mineralization of 14C-labelled sulfamethoxazole under
570 different redox conditions. Science of Total Environment 542, 706–715.

571 Alvarino, T., Suárez, S., Katsou, E., Vazquez-Padin, J., Lema, J.M., Omil, F., 2015. Removal of
572 PPCPs from the sludge supernatant in a one stage nitritation/anammox process. Water
573 Research. 68, 701–709. d

574 Anthony, C., 1982. The Biochemistry of Methylotrophs. Academic Press. London

575 Anthony, C., 2011. How half a century of research was required to understand bacterial growth on
576 C1 and C2 compounds; the story of the serine cycle and the ethylmalonyl-CoA pathway.
577 Science. Progress. 94, 109–37.

578 Bassin, J.P., Abbas, B., Vilela, C.L.S., Kleerebezem, R., Muyzer, G., Rosado, a. S., van
579 Loosdrecht, M.C.M., Dezotti, M., 2015. Tracking the dynamics of heterotrophs and nitrifiers
580 in moving-bed biofilm reactors operated at different COD/N ratios. Bioresource Technology
581 192 (3), 131–141.

582 Baytshtok, V., Lu, H., Park, H., Kim, S., Yu, R., Chandran, K., 2009. Impact of varying electron
583 donors on the molecular microbial ecology and biokinetics of methylotrophic denitrifying
584 bacteria. Biotechnology and Bioengineering 102 (6), 1527–1536.

585 Beun, J.J., Paletta, F., Van Loosdrecht, M.C., Heijnen, J.J., 2000. Stoichiometry and kinetics of
586 poly-beta-hydroxybutyrate metabolism in aerobic, slow growing, activated sludge cultures.
587 Biotechnology and Bioengineering 67 (4), 379–89.

588 Biswas, K., Turner, S.J., 2012. Microbial community composition and dynamics of moving bed
589 biofilm reactor systems treating municipal sewage. Applied Environmental Microbiology 78
590 (3), 855–64.

591 Christensson, M., Lie, E., Welander, T., 1944. A comparison between ethanol and methanol as
592 carbon sources for denitrification. Water Science and Technology 30 (6), 83-90.

593 Clara, M., Strenn, B., Gans, O., Martinez, E., Kreuzinger, N., Kroiss, H., 2005. Removal of selected
594 pharmaceuticals, fragrances and endocrine disrupting compounds in a membrane bioreactor
595 and conventional wastewater treatment plants. Water Research 39 (19), 4797–807.

596 Criddle, C.S., 1993. The kinetics of cometabolism. Biotechnology and Bioengineering 41 (11),
597 1048–56.

598 Cumming, G., Fidler, F., Vaux, D.L., 2007. Error bars in experimental biology. Journal of Cell
599 Biology 177 (1), 7–11.

600 Dawas-Massalha, A., Gur-Reznik, S., Lerman, S., Sabbah, I., Dosoretz, C.G., 2014. Co-metabolic
601 oxidation of pharmaceutical compounds by a nitrifying bacterial enrichment. Bioresource and
602 Technology. 167, 336–42.

603 Delgadillo-Mirquez, L., Lardon, L., Steyer, J.P., Patureau, D., 2011. A new dynamic model for
604 bioavailability and cometabolism of micropollutants during anaerobic digestion. Water
605 Research 45 (15), 4511–4521.

606 Daughton, C.G., Ternes, T.A., 1999. Pharmaceuticals and personal care products in the
607 environment: agents of subtle change? Environmental Health Perspectives. 907–38.

608 Escolà Casas, M.E., Chhetri, R.K., Ooi, G., Hansen, K.M.S., Litty, K., Christensson, M.,
609 Kragelund, C., Andersen, H.R., Bester, K., 2015a. Biodegradation of pharmaceuticals in
610 hospital wastewater by staged Moving Bed Biofilm Reactors (MBBR). Water Research. 83,
611 293–302.

612 Escolà Casas, M., Chhetri, R.K., Ooi, G., Hansen, K.M.S., Litty, K., Christensson, M., Kragelund,
613 C., Andersen, H.R., Bester, K., 2015b. Biodegradation of pharmaceuticals in hospital
614 wastewater by a hybrid biofilm and activated sludge system (Hybas). Science of Total
615 Environment. 530-531, 383–392.

616 Falås, P., Baillon-Dhumez, A, Andersen, H.R., Ledin, A la Cour Jansen, J., 2012. Suspended
617 biofilm carrier and activated sludge removal of acidic pharmaceuticals. Water Research. 46
618 (4), 1167–75.

619 Falås, P., Longrée, P., la Cour Jansen, J., Siegrist, H., Hollender, J., Joss, A, 2013. Micropollutant
620 removal by attached and suspended growth in a hybrid biofilm-activated sludge process. Water
621 Research 47 (13), 4498–506.

622 Fernandez-Fontaina, E., Carballa, M., Omil, F., Lema, J.M., 2014. Modelling cometabolic
623 biotransformation of organic micropollutants in nitrifying reactors. Water Research 65C, 371–
624 383.

625 Fischer, K., Majewsky, M., 2014. Cometabolic degradation of organic wastewater micropollutants
626 by activated sludge and sludge-inherent microorganisms. Applied Microbiology and

627 Biotechnology 98 (15), 6583–97.

628 Göbel, A., McArdell, C.S., Joss, A., Siegrist, H., Giger, W., 2007. Fate of sulfonamides,
629 macrolides, and trimethoprim in different wastewater treatment technologies. Science of Total
630 Environment 372 (2-3), 361–371.

631 Hagman, M., Nielsen, J.L., Nielsen, P.H., La, J., Jansen, C., 2007. Mixed carbon sources for nitrate
632 reduction in activated sludge-identification of bacteria and process activity studies. Water
633 Environmen Research 42, 1539–1546

634 Hallin, S., Throbäck, I.N., Dicksved, J., Pell, M., 2006. Metabolic profiles and genetic diversity of
635 denitrifying communities in activated sludge after addition of methanol or ethanol. Applied
636 Microbiology and Biotechnology 72 (8), 5445–52.

637 Hapeshi, E., Lambrianides, A., Koutsoftas, P., Kastanos, E., Michael, C., Fatta-Kassinos, D., 2013.
638 Investigating the fate of iodinated X-ray contrast media iohexol and diatrizoate during
639 microbial degradation in an MBBR system treating urban wastewater. Environmental Science
640 and Pollution Research 20 (6), 3592–606.

641 Hiatt, W.C., Grady, C.P.L., 2008. An Updated Process Model for Carbon Oxidation, Nitrification,
642 and Denitrification. Water Environmen Research 80 (11), 2145–2156.

643 Hill, M., 1973. Diversity and evenness: a unifying notation and its consequences. Ecology 54 (2),
644 427–432.

645 Jenkins, O., Byrom, D., Jones, D., 1987. Methylophilus - a New Genus of Methanol-Utilizing
646 Bacteria. International Journal of Systematic Bacteriology. 37 (4), 446–448.

647 Johnson, D.R., Helbling, D.E., Lee, T.K., Park, J., Fenner, K., Kohler, H.P.E., Ackermann, M.,
648 2015. Association of biodiversity with the rates of micropollutant biotransformations among
649 full-scale wastewater treatment plant communities. Applied and Environmental Microbiology
650 81 (2), 666–675.

651 Joss, A., Siegrist, H., Ternes, T.A., 2008. Are we about to upgrade wastewater treatment for
652 removing organic micropollutants? Water Science and Technology 57, 251–5.

653 Joss, A., Zabczynski, S., Göbel, A., Hoffmann, B., Löffler, D., McArdell, C.S., Ternes, T. a.,
654 Thomsen, A., Siegrist, H., 2006. Biological degradation of pharmaceuticals in municipal
655 wastewater treatment: Proposing a classification scheme. Water Research 40 (8), 1686–1696.

656 Kassotaki, E., Buttiglieri, G., Ferrando-Climent, L., Rodriguez-Roda, I., Pijuan, M., 2016.
657 Enhanced sulfamethoxazole degradation through ammonia oxidizing bacteria co-metabolism
658 and fate of transformation products. Water Research.

659 Liu, L., Binning, P.J., Smets, B.F., 2015. Evaluating alternate biokinetic models for trace pollutant
660 cometabolism. Environmental Science and Technology 49 (4), 2230–2236.

661 Louzeiro, N., 2002. Methanol-induced biological nutrient removal kinetics in a full-scale
662 sequencing batch reactor. Water Research. 36 (11), 2721–2732.

663 Lu, H., Chandran, K., Stensel, D., 2014. Microbial ecology of denitrification in biological
664 wastewater treatment. Water Research. 64, 237–254.

665 Luo, Y., Guo, W., Ngo, H.H., Nghiem, L.D., Hai, F.I., Kang, J., Xia, S., Zhang, Z., Price, W.E.,
666 2014. Removal and fate of micropollutants in a sponge-based moving bed bioreactor.
667 Bioresource Technology 159, 311–9.

668 Maurer, M., Escher, B.I., Richle, P., Schaffner, C., Alder, a C., 2007. Elimination of beta-blockers
669 in sewage treatment plants. Water Research. 41 (7), 1614–22.

670 Mazioti, A. a., Stasinakis, A.S., Pantazi, Y., Andersen, H.R., 2015. Biodegradation of
671 benzotriazoles and hydroxy-benzothiazole in wastewater by activated sludge and moving bed
672 biofilm reactor systems. Bioresource Technology 192, 627–635.

673 Mokhayeri, Y., Riffat, R., Murthy, S., Bailey, W., Takacs, I., Bott, C., 2009. Balancing yield,
674 kinetics and cost for three external carbon sources used for suspended growth post-
675 denitrification. Water Science and Technology 60, 2485–91.

676 Müller, E., Schüssler, W., Horn, H., Lemmer, H., 2013. Aerobic biodegradation of the sulfonamide
677 antibiotic sulfamethoxazole by activated sludge applied as co-substrate and sole carbon and
678 nitrogen source. Chemosphere 92, 969–78.

679 Onesios, K.M., Yu, J.T., Bouwer, E.J., 2009. Biodegradation and removal of pharmaceuticals and
680 personal care products in treatment systems: a review. Biodegradation 20 (4), 441–466.

681 Pan, Y., Ni, B.-J., Lu, H., Chandran, K., Richardson, D., Yuan, Z., 2015. Evaluating two concepts
682 for the modelling of intermediates accumulation during biological denitrification in wastewater
683 treatment. Water Research. 71, 21–31.

684 Petrie, B., McAdam, E.J., Lester, J.N., Cartmell, E., 2014. Assessing potential modifications to the
685 activated sludge process to improve simultaneous removal of a diverse range of
686 micropollutants. Water Research, 180-92.

687 Plósz, B.G., Benedetti, L., Daigger, G.T., Langford, K.H., Larsen, H.F., Monteith, H., Ort, C., Seth,
688 R., Steyer, J.-P., Vanrolleghem, P. a, 2013. Modelling micro-pollutant fate in wastewater

689 collection and treatment systems: status and challenges. Water Science and Technology 67, 1–
690 15.

691 Plósz, B.G., Langford, K.H., Thomas, K. V, 2012. An activated sludge modeling framework for
692 xenobiotic trace chemicals (ASM-X): assessment of diclofenac and carbamazepine.
693 Biotechnology and Bioengineering 109 (11), 2757–69.

694 Plósz, B.G., Leknes, H., Thomas, K. V, 2010. Impacts of competitive inhibition, parent compound
695 formation and partitioning behavior on the removal of antibiotics in municipal wastewater
696 treatment. Environmental Science and Technology 44 (2), 734–42.

697 Polesel, F., Andersen, H.R., Trapp, S., Plosz, B.G., 2016. Removal of antibiotics in biological
698 wastewater treatment systems – A critical assessment using the Activated Sludge Modelling
699 framework for Xenobiotics (ASM-X). Environmental Science and Technology 50 (19),
700 10316–10334

701 Popat, S.C., Deshusses, M.A., 2011. Kinetics and inhibition of reductive dechlorination of
702 trichloroethene, cis-1,2-dichloroethene and vinyl chloride in a continuously fed anaerobic
703 biofilm reactor. Environmental Science and Technology 45 (84), 1569–1578.

704 Reichert, P., 1994. Aquasim - a tool for simulation and data-analysis of aquatic systems. Water
705 Science and Technology 30 (2), 21 – 30.

706 Rittmann, B.E., 1992. Microbiological detoxification of hazardous organic contaminants : the
707 crucial role of substrate interactions. Water Science and Technology 25, 403–410.

708 Roeleveld, P.J., Van Loosdrecht, M.C.M., 2002. Experience with guidelines for wastewater
709 characterisation in The Netherlands. Water Science and Technology 45 (6), 77–87.

710 Santos, S.G., Zaiat, M., Varesche, M.B., Foresti, E., 2001. Comparative research on the use of
711 methanol , ethanol and methane as electron donors for denitrification. Environmental
712 Engineering Science 21 (39), 313-320.

713 Sözen, S., Çokgör, E.U., Orhon, D., Henze, M., 1998. Respirometric analysis of activated sludge
714 behaviour—II. Heterotrophic growth under aerobic and anoxic conditions. Water Research. 32,
715 476–488.

716 Stadler, L.B., Love, N.G., 2016. Impact of microbial physiology and microbial community structure
717 on pharmaceutical fate driven by dissolved oxygen concentration in nitrifying bioreactors.
718 Water Research. 104, 189–199.

719 Su, L., Aga, D., Chandran, K., Khunjar, W.O., 2015. Factors impacting biotransformation kinetics
720 of trace organic compounds in lab-scale activated sludge systems performing nitrification and
721 denitrification. Journal Hazardaus Material 282, 116–24.

722 Suárez, S., Lema, J.M., Omil, F., 2010. Removal of Pharmaceutical and Personal Care Products (
723 PPCPs) under nitrifying and denitrifying conditions. Water Research 44 (10), 3214–3224.

724 Suárez, S., Ramil, M., Omil, F., Lema, J.M., 2005. Removal of pharmaceutically active compounds
725 in nitrifying-denitrifying plants. Water Science and Technology 52 (8), 9–14.

726 Suárez, S., Reif, R., Lema, J.M., Omil, F., 2012. Mass balance of pharmaceutical and personal care
727 products in a pilot-scale single-sludge system: influence of T, SRT and recirculation ratio.
728 Chemosphere 89 (2), 164–71.

729 Torresi, E., Fowler, J.S., Polesel, F., Bester, K., Andersen, H.R., Smets, B.F., Plosz, B.G.,
730 Christensson, M., 2016. Biofilm thickness influences biodiversity in nitrifying MBBRs –

731 Implications on micropollutant removal. Environmental Science and Technology. 50 (17),
732 9279–9288

733 Tran, N.H., Urase, T., Kusakabe, O., 2009. The characteristics of enriched nitrifier culture in the
734 degradation of selected pharmaceutically active compounds. Journal of Hazardous Material
735 171 (1-3), 1051–7.

736 Tran, N.H., Urase, T., Ngo, H.H., Hu, J., Ong, S.L., 2013. Insight into metabolic and cometabolic
737 activities of autotrophic and heterotrophic microorganisms in the biodegradation of emerging
738 trace organic contaminants. Bioresource Technology. 146, 721–31.

739 Vree, T.B., de Ven, E.S. van, Verwey-van Wissen, C.P.W.G.M., Baars, A.M., Swolfs, A., van
740 Galen, P.M., Amatdjais-Groenen, H., 1995. Isolation, identification and determination of
741 sulfadiazine and its hydroxy metabolites and conjugates from man and Rhesus monkey by
742 high-performance liquid chromatography. Journal of Chromatography B: Biomedical Sciences
743 and Applications 670 (1), 111–123.

744 Wittebolle, L., Marzorati, M., Clement, L., Balloi, A., Daffonchio, D., Heylen, K., De Vos, P.,
745 Verstraete, W., Boon, N., 2009. Initial community evenness favours functionality under
746 selective stress. Nature 458 (72238), 623–6.

747 Xia, S., Jia, R., Feng, F., Xie, K., Li, H., Jing, D., Xu, X., 2012. Effect of solids retention time on
748 antibiotics removal performance and microbial communities in an A/O-MBR process.
749 Bioresource Technology. 106, 36–43.

750 Zarfl, C., Klasmeier, J., Matthies, M., 2009. A conceptual model describing the fate of sulfadiazine
751 and its metabolites observed in manure-amended soils. Chemosphere 77 (6), 720–726.

752 Zupanc, M., Kosjek, T., Petkovšek, M., Dular, M., Kompare, B., Širok, B., Blažeka, Ž., Heath, E.,
753 2013. Removal of pharmaceuticals from wastewater by biological processes, hydrodynamic
754 cavitation and UV treatment. Ultrason. Sonochem. 20, 1104–12.

755

756

757

758 **Web references**

759 EAWAG-BBD Pathway Prediction System. http://eawag-bbd.ethz.ch/predict/index.html (Accessed
760 February 24, 2016). (2016)

761

Tables

Table 1. Stoichiometric (Gujer) matrix of the ASM-X (which includes processes such as parent compound retransformation, biotransformation and the cometabolic model) and two-step denitrifying model used in this study.
Stoichiometric coefficients: A= (1-Y_H)/(1.143 * Y_H); B = (1-Y_H)/(1.713 * Y_H); F = ratio between molecular mass of parent compound and metabolite undergoing deconjugation. Parameters and state variables for determination of micropollutant kinetics are described in the main text. Parameters and state variables for the denitrifying model are defined in Table S1 in Supplementary Information. For estimation of denitrification kinetics, biomass concentration X_H is expressed in gCOD L^{-1}; *Due to short duration of the batch experiment and low S/X ratio, negligible biomass growth was assumed.

(i) Component → i (j)Processes ↓	C_{LI}	C_{CJ}	S_{NO3}	S_{NO2}	S_{N2}	S_s	$X_{biomass}$	Process rate
Micropollutants kinetics								
(1)Parent compound retransformation	F	-1						$\frac{k_{Dec} C_{CJ} X_{biomass}}{1+K_D X_{biomass}}$
(2)Biotransformation	-1							$\frac{k_{bio} C_{LI} X_{biomass}}{1+K_D X_{biomass}}$
(3)Cometabolism	-1							$\frac{q_{bio}(Ss/(Ss+K_S))+k_{bio}}{1+K_D X_{biomass}} C_{LI} X_{biomass}$
Denitrification kinetics								
R1			-A	+A		-1/Y_H	*	$\mu_H \eta_{g1} X_H \frac{Ss}{K_{S1}+S_S} \frac{S_{NO3}}{K_{NO3}^{HB}+S_{NO3}}$
R2				-B	+B	-1/Y_H	*	$\mu_H \eta_{g2} X_H \frac{Ss}{K_{S2}+S_S} \frac{S_{NO2}}{K_{NO2}^{HB}+S_{NO2}}$

R1: Anoxic growth of heterotrophs, reducing nitrate to nitrite (NO_3^- -> NO_2^-)
R2: Anoxic growth of heterotrophs, reducing nitrite to nitrogen (NO_2^- -> N_2)

775 **Table 2. Values of denitrification rates normalized by carriers surface area ($r_{NO3,2-N}$) and biomass**
776 **concentration ($k_{NO3,2-N}$) measured during batch experiments. SA: total surface area of carriers in the**
777 **MBBRs.**
778

MBBR	SA (m^2)	Biomass ($g\ L^{-1}$)	$r_{NO3,2}$-N ($gNO_{3,2}$-N $m^{-2}\ d^{-1}$)	$k_{NO3,2}$-N ($gNO_{3,2}$-N $g_{biomass}^{-1}\ d^{-1}$)
Methanol-dosed	0.2	3.28 ±0.93	1.77 ± 0.92	0.11 ± 0.06
Ethanol-dosed	0.2	4.20 ±0.25	2.32 ± 0.62	0.11 ± 0.03

779

780

781 **Table 3. Values of k, k_{bio}, q_{bio} and k_{Dec} estimated for the two MBBRs from the data obtained in the**
782 **batch experiments. "k" defines the removal rate constant obtained following single first-order**
783 **kinetics and not accounting for biomass concentration and sorption processes. "k_{bio}" and "q_{bio}" refer**
784 **to removal rate constants normalized for biomass and sorption processes. Unindexed values**
785 **correspond to "k_{bio}" (Biotransformation process, Table 1, Process 2). Index (1) indicates the case of**
786 **retransformation rate constant "k_{Dec}" of acetyl-sulfadiazine to sulfadiazine (Transformation process,**
787 **Table 1, Process 1). Index (2) refers to the cometabolic rate constant "q_{bio}" (Cometabolism, Table 1,**
788 **Process 3). The following abbreviations are used: n.d. = not degradable, SD =standard deviation.**
789

	Methanol-dosed MBBR		Ethanol-dosed MBBR	
Compound	k ± SD (d^{-1})	k_{bio}, q_{bio} ± SD ($L\ d^{-1} g_{biomass}^{-1}$)	k ± SD (d^{-1})	k_{bio}, q_{bio} ± SD ($Ld^{-1} g_{biomass}^{-1}$)
Easily degradable; k_{bio}, q_{bio} >2				
Propranolol	17.8 ± 0.2	12.9 ± 1.3	17.7 ± 0.2	11.7 ± 0.7
Atenolol	17.8 ± 0.2	6.4 ± 0.6	17.6 ± 0.2	5.1 ± 0.3
Citalopram	14.2 ± 0.9	4.3 ± 0.5	12.3 ± 0.1	2.3 ± 0.1
Trimethoprim	13.6 ± 0.1	4.1 ± 0.4	9.0 ± 0.1	2.1 ± 0.1
Acetyl-sulfadiazine	12.1± 0.3	3.7 ± 0.4 (1)	17.6 ± 0.2	4.2 ± 0.3 (1)
Moderately degradable; 0.2 ≤ k_{bio}, q_{bio} ≤2				
Ibuprofen	4.6 ± 0.1	1.4 ± 0.4	2.3 ± 0.1	0.5 ± 0.03
Clarithromycin	2.9 ± 0.7	1.0 ± 0.2 (2) 0.6 ± 0.1	4.4 ± 0.9	0.9 ± 0.2(2) 0.4 ± 0.1
Iopromide	3.0 ± 0.1	0.9 ± 0.1	1.7 ± 0.1	0.4 ± 0.1
Metoprolol	2.6 ± 0.1	0.8 ± 0.2	1.7 ± 0.1	0.4 ± 0.03
Iohexol	2.3 ± 0.1	0.7 ± 0.2	1.2 ± 0.1	0.3 ± 0.1
Iomeprol	2.1 ± 0.1	0.6 ± 0.1	1.2 ± 0.1	0.3 ± 0.1
Sotalol	1.3 ± 0.1	0.5 ± 0.1	0.7 ± 0.1	0.2 ± 0.02
Erythromycin	1.5 ± 0.1	0.5 ± 0.1 (2) 0.2 ± 0.1	2.5 ± 0.1	0.6 ± 0.1(2) 0.2 ± 0.1
Venlafaxine	6.0 ± 0.1	1.9 ± 0.2 (2) 0.1 ± 0.1	4.8 ± 0.1	1.1 ± 0.1(2) 0.1 ± 0.1
Carbamazepine	3.9 ± 0.1	1.2 ± 0.3 (2) 0.1 ± 0.1	4.6 ± 0.1	1.1 ± 0.1(2) 0.1 ± 0.1
Sulfamethoxazole	5.6 ± 0.8	1.7 ± 0.2 (2) 0.1 ± 0.1	13.5 ± 0.7	3.2 ± 0.2 (2) 0.1 ± 0.1
Sulfamethizole	5.8 ± 0.9	1.8 ± 0.2 (2) 0.1 ± 0.1	13.8 ± 0.8	3.3 ± 0.2 (2) 0
Sulfadiazine	1.9 ± 0.2	0.6 ± 0.1	4.2 ± 0.6	1.0 ± 0.2
Hardly or non-degradable; k_{bio}, q_{bio} <0.2				
Diatrizoic acid	0.3 ± 0.1	0.1 ± 0.02	0.1 ± 0.1	0.1 ± 0.1
Iopamidol	0.2 ± 0.1	0.1 ± 0.02	0.1 ± 0.1	0.1 ± 0.1
Diclofenac	n.d.	n.d.	n.d.	n.d.
Phenazone	n.d.	n.d.	n.d.	n.d.

790

Figures

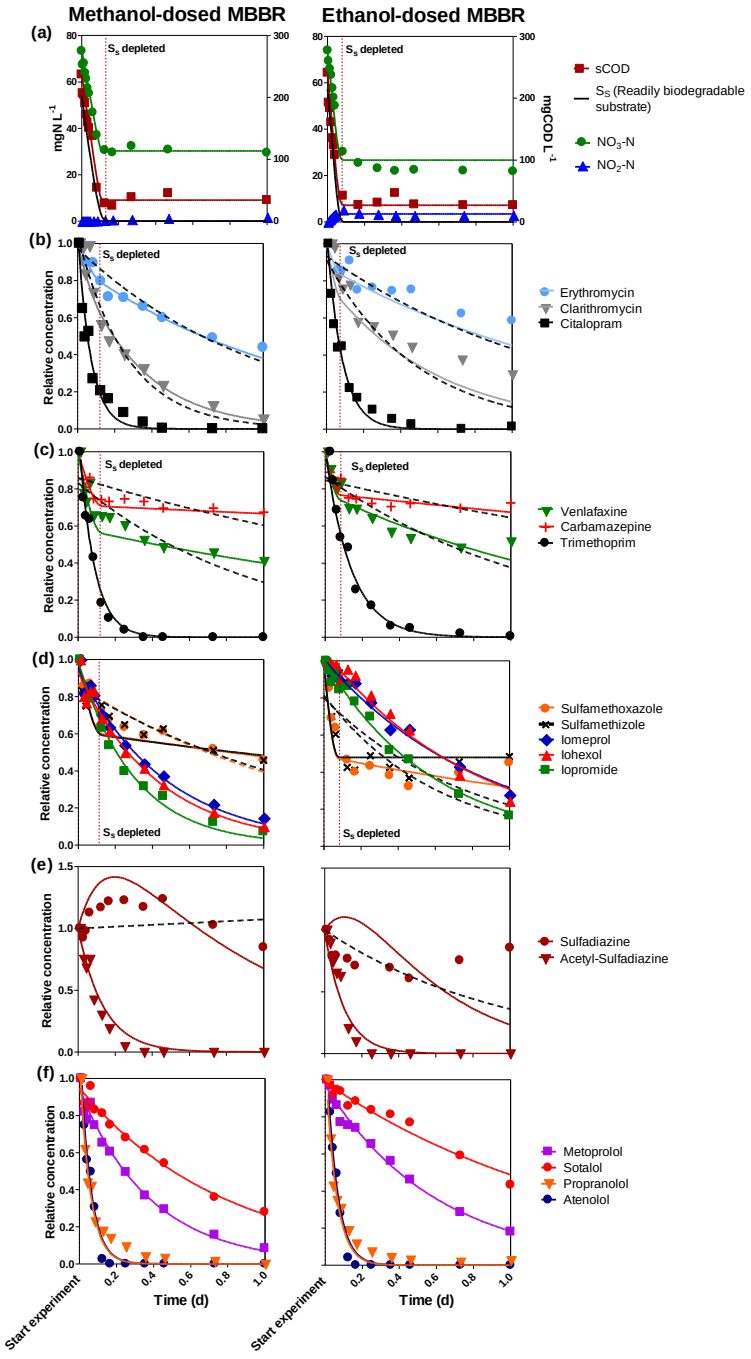

Figure 1. Batch experiment results for selected compounds. On the X-axes "Time (d)" designates the sampling time-points. On the Y-axes "Relative concentration" refers to concentrations normalized to the measured starting concentrations. Symbols refer to measurements while lines refer to modelling. [a] Macro-pollutants. Readily biodegradable substrate (S_S) is only modelled. [b-d] Solid lines: modelled concentrations assuming cometabolism (process 3, Table 1). Dashed lines: concentrations according to the biotransformation model (process 2, Table 1). [e] Solid lines: biotransformation-retransformation model (process 1, Table 1) assuming deconjugation of acetyl-sulfadiazine to sulfadiazine. Dashed lines: biotransformation model (process 2, Table 1),. [f] Solid lines: concentrations according to the biotransformation model (process 2, Table 1).

802

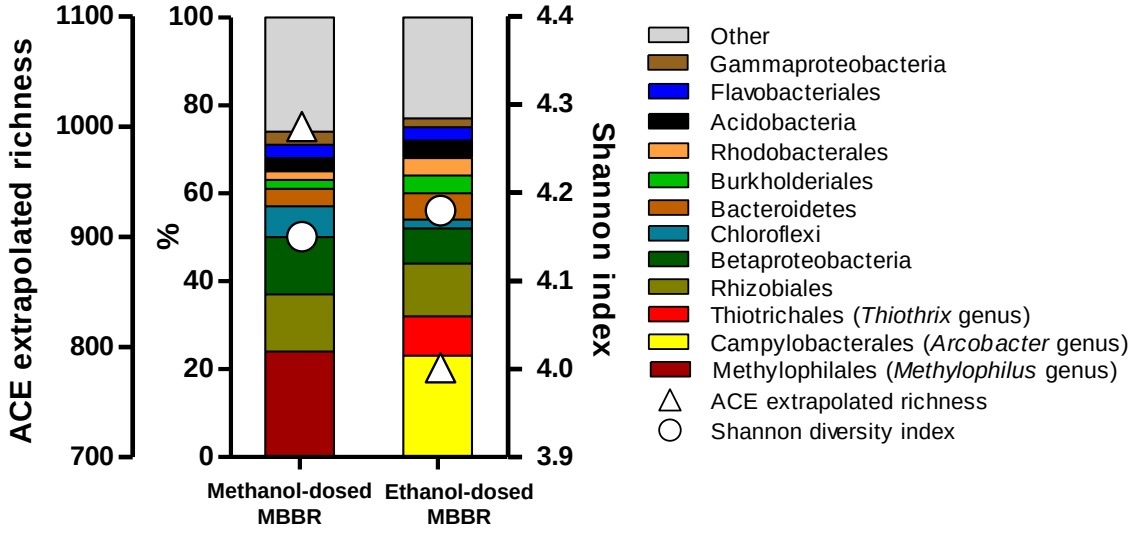

803

804 **Figure 2. Order-level taxonomic classification of 16S rRNA amplicons of the two MBBRs. The three**
805 **most abundant orders are reported also at genus level (*Methylophiulus*, *Arcobacter* and *Thiotrix*).**
806 **Taxa abundance is expressed in percentage (second left axis). Alpha-diversity is measured as ACE**
807 **extrapolated richness (first left axis) and Shannon diversity index (right axis).**

808

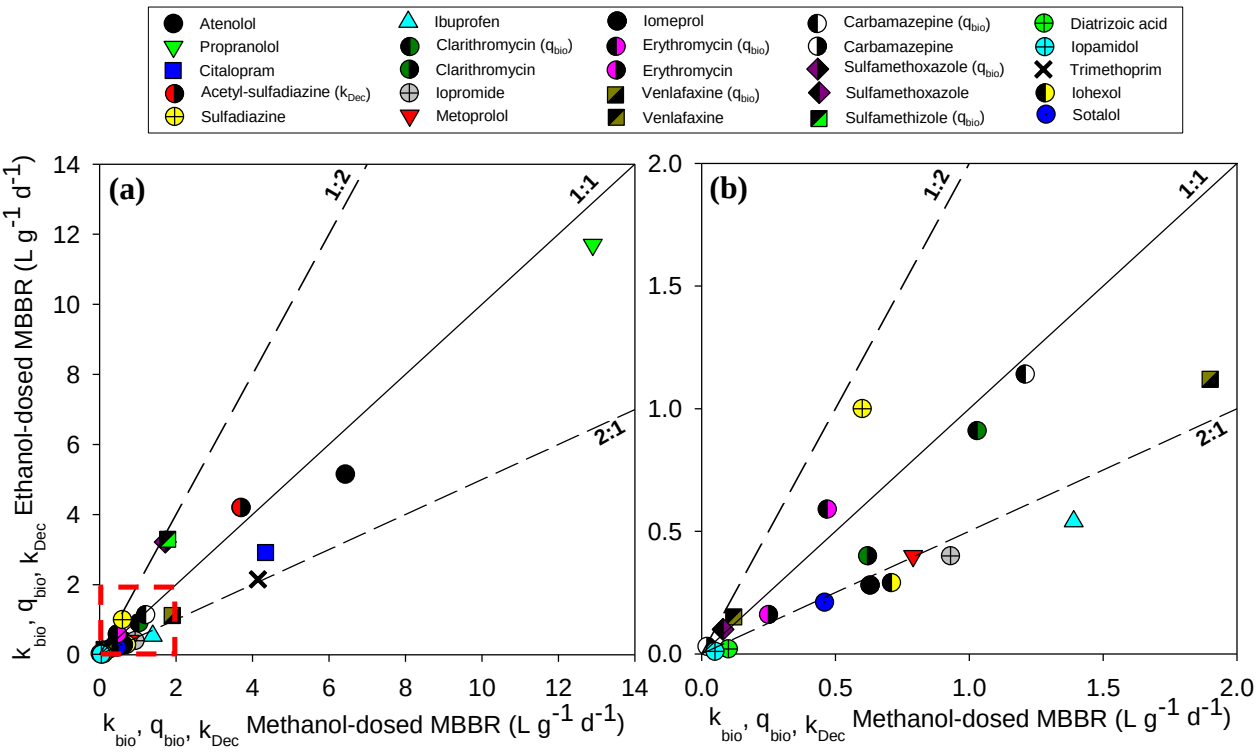

Figure 3. Comparative assessment between methanol-dosed reactor (x-axes) and the ethanol-dosed reactor (y-axes) of the removal kinetics $k_{bio,}$ q_{bio} and k_{Dec} estimated for all targeted compounds (a) and for compounds with biokinetics ranging between 0 and 2 L $g_{biomass}^{-1}$ d^{-1} (b). Dashed lines (2:1 and 1:2) delimit area where biokinetics are 2-folder higher or lower than other estimated values. In the legend, when not specified, symbols refer to estimated k_{bio}.

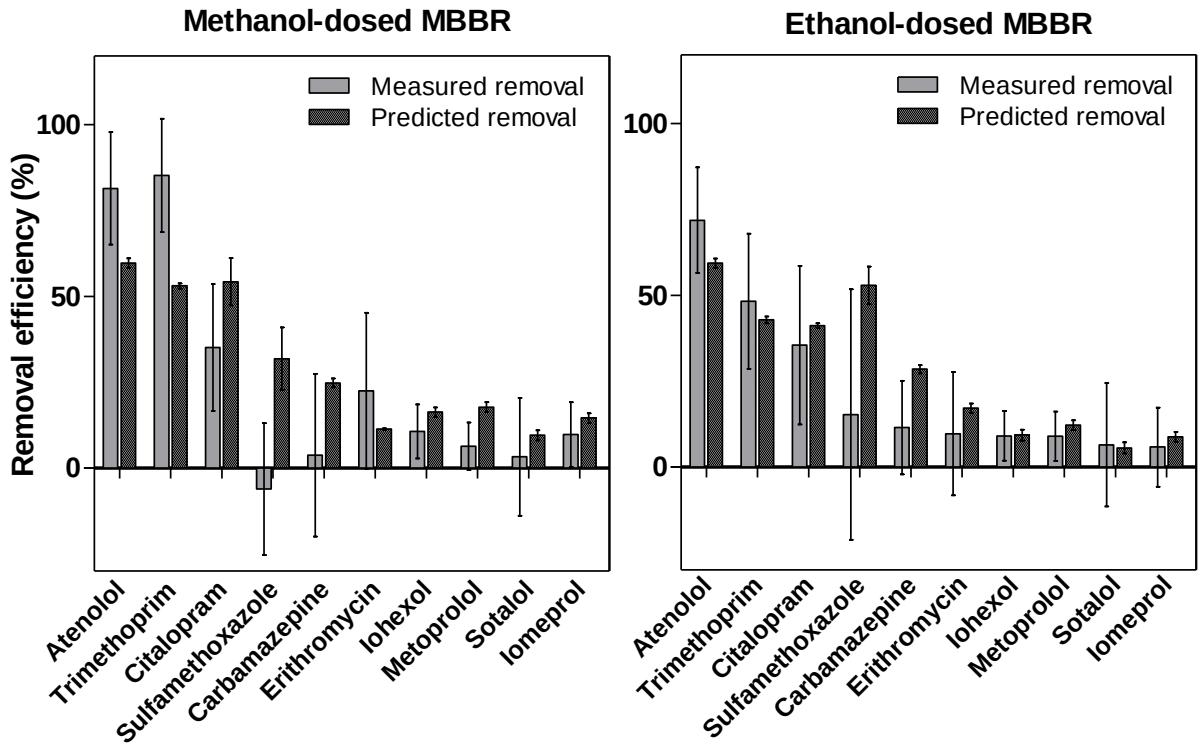

Figure 4. Measured mean removal efficiency of micropollutants of all the tested COD_{added}/NO^3-N influent ratios (presented in Table S3, SI) during the whole continuous-flow experiment, taking into account that no correlation was found between micropollutant removal and COD_{added}/NO^3-N influent ratios. The measured removals were calculated as difference between influent and effluent concentration, expressed as a percentage. Predicted removal was based on removal rate constants k (d^{-1}) derived from batch experiments, calculated according to Equation 1 in Section 2.6.